Application of Computational Intelligence in Describing the Drying Kinetics of Persimmon Fruit (Diospyros kaki) During Vacuum and Hot Air Drying Process

Authors:

Alfadhl Yahya Khaled, Abraham Kabutey, Kemal Ça?atay Selvi, ?estmír Mizera, Petr Hrabe, David Herák

Date Submitted: 2020-07-07

Keywords: support vector machine model, k-nearest neighbors, artificial neural network model, computational intelligence methods, drying methods, persimmon fruit

Abstract:

This study examines the potential of applying computational intelligence modelling to describe the drying kinetics of persimmon fruit slices during vacuum drying (VD) and hot-air-drying (HAD) under different drying temperatures of 50 °C, 60 °C and 70 °C and samples thicknesses of 5 mm and 8 mm. Kinetic models were developed using selected thin layer models and computational intelligence methods including multi-layer feed-forward artificial neural network (ANN), support vector machine (SVM) and k-nearest neighbors (kNN). The statistical indicators of the coefficient of determination (R2) and root mean square error (RMSE) were used to evaluate the suitability of the models. The effective moisture diffusivity and activation energy varied between 1.417 × 10?9 m2/s and 1.925 × 10?8 m2/s and 34.1560 kJ/mol to 64.2895 kJ/mol, respectively. The thin-layer models illustrated that page and logarithmic model can adequately describe the drying kinetics of persimmon sliced samples with R2 values (>0.9900) and lowest RMSE (<0.0200). The ANN, SVM and kNN models showed R2 and RMSE values of 0.9994, 1.0000, 0.9327, 0.0124, 0.0004 and 0.1271, respectively. The validation results indicated good agreement between the predicted values obtained from the computational intelligence methods and the experimental moisture ratio data. Based on the study results, computational intelligence methods can reliably be used to describe the drying kinetics of persimmon fruit.

Record Type: Published Article

Submitted To: LAPSE (Living Archive for Process Systems Engineering)

Citation (overall record, always the latest version):	LAPSE:2020.0812
Citation (this specific file, latest version):	LAPSE:2020.0812-1
Citation (this specific file, this version):	LAPSE:2020.0812-1v1

DOI of Published Version: https://doi.org/10.3390/pr8050544

processes

MDPI

Article

Application of Computational Intelligence in Describing the Drying Kinetics of Persimmon Fruit (*Diospyros kaki*) During Vacuum and Hot Air Drying Process

Alfadhl Yahya Khaled [1,*], Abraham Kabutey [1], Kemal Çağatay Selvi [1], Čestmír Mizera [1], Petr Hrabe [2] and David Herák [1]

1 Department of Mechanical Engineering, Faculty of Engineering, Czech University of Life Sciences Prague, Kamýcká 129, 165 00 Prague, Czech Republic; kabutey@tf.czu.cz (A.K.); kcselvi74@gmail.com (K.Ç.S.); mizera@tf.czu.cz (Č.M.); herak@tf.czu.cz (D.H.)

2 Department of Material Science and Manufacturing Technology, Faculty of Engineering, Czech University of Life Sciences Prague, Kamýcká 129, 165 00 Prague, Czech Republic; hrabe@tf.czu.cz

* Correspondence: f_yahya87@hotmail.com; Tel.: +420-7763-17207

Received: 23 March 2020; Accepted: 28 April 2020; Published: 7 May 2020

Abstract: This study examines the potential of applying computational intelligence modelling to describe the drying kinetics of persimmon fruit slices during vacuum drying (VD) and hot-air-drying (HAD) under different drying temperatures of 50 °C, 60 °C and 70 °C and samples thicknesses of 5 mm and 8 mm. Kinetic models were developed using selected thin layer models and computational intelligence methods including multi-layer feed-forward artificial neural network (ANN), support vector machine (SVM) and k-nearest neighbors (kNN). The statistical indicators of the coefficient of determination (R^2) and root mean square error (RMSE) were used to evaluate the suitability of the models. The effective moisture diffusivity and activation energy varied between 1.417×10^{-9} m^2/s and 1.925×10^{-8} m^2/s and 34.1560 kJ/mol to 64.2895 kJ/mol, respectively. The thin-layer models illustrated that page and logarithmic model can adequately describe the drying kinetics of persimmon sliced samples with R^2 values (>0.9900) and lowest RMSE (<0.0200). The ANN, SVM and kNN models showed R^2 and RMSE values of 0.9994, 1.0000, 0.9327, 0.0124, 0.0004 and 0.1271, respectively. The validation results indicated good agreement between the predicted values obtained from the computational intelligence methods and the experimental moisture ratio data. Based on the study results, computational intelligence methods can reliably be used to describe the drying kinetics of persimmon fruit.

Keywords: persimmon fruit; drying methods; computational intelligence methods; artificial neural network model; support vector machine model; k-nearest neighbors

1. Introduction

Persimmon (*Diospyros kaki*) is an edible fruit with a sweet taste and rich in vitamin A, C, calcium, condensed tannins, carotenoid, phenolic compounds and iron [1–3]. Besides the nutritional value of persimmon, it has many health benefits such as therapeutic effect on cardiovascular system disease, helps effectively to reduce cholesterol and blood pressure, strengthens the immune system, prevents cancer and remedy for digestion [4]. Persimmon has high moisture content resulting in susceptibility to spoilage even at refrigerator temperatures. Thus, it has to be preserved by proper drying processes to increase the shelf life [5,6].

Drying is considered one of the commonly used postharvest preservation techniques. The drying process of harvested agricultural products assists in reducing spoilage, increasing shelf-life and reducing the bulk weight of products during transportation. Drying of agricultural products causes the enzymatic reactions to be inactivated as a result of heat and mass transfer leading to a reduction of the moisture content inside the product [7]. It also helps the extraction of bioactive compounds from food products. Drying methods such as hot-air drying (HAD), freeze-drying (FD), vacuum drying (VD), microwave drying (MWD) and infrared drying (IRD) have been used in drying agricultural crops [7–10]. Amongst these drying methods, the HAD and VD are the most common commercially used drying methods as they provide more uniform dried product, naturally harmless and nontoxic [11]. For the VD method, the use of low temperatures in the absence of oxygen can preserve heat-sensitive and easily oxidizable foods [12]. Consequently, discoloration and decomposition of the flavor and some nutritional substances can be prevented [10]. However, using HAD and VD without appropriate operating parameters can negatively affect the essential properties of food products such as nutritional and phytochemical properties. Hence, the determination of the optimum operating parameters, drying conditions using suitable drying models are indispensable for achieving quality along with minimum product cost and maximum yield [7,13,14].

Previous studies have explored several mathematical thin-layer drying models (empirical, semi-theoretical and theoretical) to describe the drying kinetics of fruits and vegetables for enhancing the overall performance of the drying process [5,15–17]. These models are derived from the physical laws that govern the process such as mass, reaction kinetics and thermodynamics. The models accuracy of a thermal process are limited to other factors like physical properties, which may vary during the thermal process. Besides that, these models can achieve satisfying regression results in comparison with experimental data in specific conditions. Nevertheless, mathematical thin-layer models are empirical in nature, do not give the physical interpretation of the drying process and they are product dependent [18].

Computational intelligence tools such as artificial neural networks (ANN), support vector machine (SVM) and k-nearest neighbors (kNN) are considered as complex tools for complex systems and dynamic modelling [19]. The application of ANN, SVM and kNN offer many advantages compared to conventional modeling techniques due to the learning ability, increased flexibility, online non-destructive measurements, reduced assumptions, suitability to the non-linear process and tolerance of incomplete data [7,13,14]. For example, ANN is inspired by the biological neural system as a useful statistical tool for nonparametric regression [19]. SVM is highly recognized in terms of its superior performance of the regression data due to its excellent performance capability when working with multi-dimensional data [20]. The kNN is an easy-to-implement algorithm that can be used to solve prediction problems [21].

Computational intelligence modelling methods can be applied as a potential alternative to mathematical thin-layer models in the drying of fruits and vegetables due to the stability and precision in case of uncertainties in the input parameters. ANN and SVM have been successfully applied in modelling and optimizing the drying processes of fruits and vegetables such as pomelo [22], ginkgo biloba seeds [13], mushroom [23], tomato [24], wood [25], celeriac slices [26], pumpkin [11], pepper [27], eggplant [28] and tea leaves [29]. The application of computational intelligence modelling methods in many areas such as cybersecurity and health-care has proven their unique ability to learn such complex data interactions [30,31]. Therefore, including these models in the drying techniques can enhance the prediction and optimization of the drying kinetics of agricultural crops. They provide a significant advantage to overcome the large errors in predictions, by automatically adapting the models until the minimum error rate. In view of this, ANN, SVM and kNN techniques can be applied to predicting and optimizing the drying kinetics of persimmon fruit under VD and HAD. It can help in the evaluation of drying parameters in real conditions, the optimization of processing conditions and the increase in the overall drying efficiency. However, this knowledge is limited in the literature regarding the application of ANN, SVM and kNN techniques in modelling the drying kinetics of persimmon fruit

under VD and HAD. Application of these models can optimize energy and quality for persimmon fruit and further minimize the required time and production cost.

The objectives of this study are to investigate the drying characteristics of persimmon fruit at different temperatures using VD and HAD, to evaluate the feasibility of applying ANN, SVM and kNN modelling as a non-destructive technique in describing the drying behavior of persimmon fruit under different drying conditions and to compare the results to mathematical thin-layer models.

2. Materials and Methods

2.1. Samples Preparation

Persimmon fruit bought from a market in Prague, Czech Republic, was used for the experiment. A total of 30 persimmon fruits were selected based on similar physical appearances (shape, color and size). Before the drying experiments, the persimmon fruits were stored in a refrigerator at 5 °C until further processing. Prior to each experiment, samples were peeled and washed under running tap water. Afterwards they were sliced into two thickness levels of 5 mm and 8 mm with a diameter of 56 mm using a Sencor slicer (SFS 4050SS, Prague, Czech Republic). The initial moisture content of the fresh samples was determined to be 3.98 kg/kg (dry basis) based on the ASABE standard by drying 25 g of selected samples at 70 °C for 24 h using the conventional oven [32].

2.2. Drying Experiments

2.2.1. Vacuum Drying (VD) Technique

The VD technique was carried out using a laboratory-scale drying unit (l 450 Gold brunn, Poland). The vacuum was regulated at a 50 mbar ultimate pressure and 2 L/s pump speed by a vacuum pump (VE 135, RoHS, Shanghai, China). However, it is worth mentioning that the pressure was monitored through the vacuum gauge which was unstable during the drying process. This problem was solved manually by fixing the pressure at approximately 50 mbar. This meant that when the pressure increased above or decreased below 50 mbar, the pump was opened for the adjustment. The VD operates by heating the samples with a conduction heat from a heater plate in the container. The vacuum pump reduces the pressure around the sample to be dried and further ensures less atmospheric pressure. This decreases the boiling point of the water inside the product and thereby increases the rate of evaporation. The sliced samples were dried at three temperatures (50 °C, 60 °C and 70 °C). Prior to the experiments, the VD was set-up to the required temperature for 30 min to enable the dryer temperature to reach equilibrium with the surrounding air temperature. The weight of the persimmon sample was measured at 1 h interval using a digital scale (HR-250AZ, A&D Company Limited) weighing balance of 252 g 0.1 mg^{-1} precision. All the drying experiments were carried-out in triplicates and the average values were used for further analyses.

2.2.2. Hot-Air Drying (HAD) Technique

A laboratory-scale convective HAD (UF 110, Memmert, Germany) was used. Similar to VD, three temperatures (50 °C, 60 °C and 70 °C) at a constant air velocity of 1.10 m/s was attained until constant weight between two successive readings. The air velocity was measured using a Thermo-Anemometer (Model 451104, EXTECH Instruments, Tainan, Taiwan; with the accuracy of 62% velocity). Before starting the experiments, the HAD was set-up to the required temperature for a half-hour to enable the dryer temperature to reach equilibrium with the surrounding air temperature. Similar to VD, the weight of the persimmon sample was measured 1 h interval using a digital scale weighing balance; whereby the samples were removed from the dryer and measured and then returned to the dryer. The experiments were conducted in triplicate and the average values used in further analyses.

2.3. Drying Kinetics

The variation in moisture content during VD and HAD techniques was expressed in the form of moisture ratio (dimensionless) as described in Equation (1).

$$\mathrm{MR} = \frac{(M_t - M_e)}{(M_o - M_e)} \tag{1}$$

where M_t, M_e and M_o are the moisture content of the samples at time t, equilibrium moisture content and initial moisture content, respectively. According to Aghbashlo et al. [33], *Me* values did not change because they were relatively low compared to M_t and M_o values, resulting in negligible error during simplification, thus, in this study, the moisture ratio was expressed as shown in Equation (2):

$$\mathrm{MR} = \frac{\mathrm{M_t}}{\mathrm{M_o}} \tag{2}$$

2.4. Effective Moisture Diffusivity

To effectively assess the behavior of the VD and HAD methods of samples, it is important to understand the mechanisms of moisture movement within the samples during drying. Fick's diffusion equation as a dimensional approach was applied due to its simplicity to describe the mass transfer of drying samples. The effective moisture diffusivity of samples for VD and HAD methods was estimated using Crank's solution [33] of Fick's diffusion equation as described in Equation (3) [16].

$$\frac{\partial M_t}{\partial \mathrm{t}} = \nabla .\left(D_{eff}\, \nabla\, M_t\right) \tag{3}$$

Assuming constant diffusion and uniform initial moisture distribution, the Crank's solution for cylindrical shaped sample is shown in Equation (4).

$$\mathrm{MR} = \frac{8}{\pi^2} \sum_{\mathrm{n}=1}^{\infty} \frac{1}{(2\mathrm{n}+1)^2} \exp\left(-\frac{(2\mathrm{n}+1)^2 D_{eff}\, \mathrm{t}}{\mathrm{r}^2}\right) \tag{4}$$

where D_{eff} is the effective moisture diffusivity (m^2/s), n is the positive integer, r is the radius of the sample (m) and t is the drying time (s). For the sake of mathematical simplicity, Equation (4) was restricted to the first term, resulting in Equation (5).

$$\mathrm{MR} = \frac{8}{\pi^2} \exp\left(-\frac{\pi^2 D_{eff}\, \mathrm{t}}{\mathrm{r}^2}\right) \tag{5}$$

2.5. Activation Energy

In general, activation energy is the minimum energy needed in order for drying to occur. The activation energies for VD and HAD methods were calculated from the relationship between effective moisture diffusivity and the average temperature of the samples based on the Arrhenius equation as shown in Equation (6) [34].

$$D_{eff} = D_o \exp\left(-\frac{E_a}{\mathrm{R}(\mathrm{T}+273.15)}\right) \tag{6}$$

where D_o is the pre-exponential factor, E_a is the activation energy (kJ/mol), R is universal gas constant (8.3143×10^{-3} kJ/mol) and T is the average temperature of the sample (K). The values of E_a for VD and HAD methods for different persimmon thickness levels were measured from the resulting slope values by plotting the fitting curve between lnD and 1/(T + 273.15) (Equation (7)).

$$\mathrm{Slope} = -\frac{E_a}{\mathrm{R}} \tag{7}$$

2.6. Mathematical Thin-Layer Modelling

The experimental drying data measured were fitted to ten selected mathematical thin-layer drying models. The selected mathematical models are listed in Table 1 namely Newton, Page, Modified page, Logarithmic, Two-term, Two-term exponential, Henderson and Pabis, Modified Henderson and Pabis, Midilli et al. and Hii et al. The coefficients of the mathematical models were determined based on non-linear least squares regression analysis using Sigma plot software (Version12.0, Systat Software Inc., California, USA). The application of these models gives a better prediction with fewer assumptions [35].

Table 1. Mathematical thin-layer drying models.

Model No.	Model Name	Model Expression	Reference
1.	Newton model	$MR = \exp(-kt)$	[36]
2.	Page model	$MR = \exp(-kt^n)$	[15]
3.	Modified page	$MR = \exp[-(kt)^n]$	[37]
4.	Logarithmic model	$MR = a\exp(-kt) + c$	[38]
5.	Two-term model	$MR = a\exp(-k_1t) + b\exp(-k_2t)$	[39]
6.	Two-term exponential model	$MR = a\exp(-k_0t) + (1-a)\exp(-k_1at)$	[40]
7.	Henderson and Pabis model	$MR = a\exp(-kt)$	[41]
8.	Modified Henderson and Pabis model	$MR = a\exp(-kt) + b\exp(-gt) + c\exp(-ht)$	[42]
9.	Midilli et al. model	$MR = a\exp(-kt) + bt$	[43]
10.	Hii et al. model	$MR = a\exp(-k_1t^n) + b\exp(-k_2t^n)$	[11]

2.7. Computational Intelligence Methods

2.7.1. Artificial Neural Network

The structure of a neural network is in the form of interconnected layers [44,45]. Haykin [46] divided an ANN into three groups of structures based on their connection namely, single layer feed-forward network, the multi-layer feed-forward network and the recurrent network. Among these structures, the multi-layer feed-forward network is widely applied in modelling of agricultural and food systems. The feed-forward neural network has an input layer (n), an output layer (m) and one or more hidden layers (h). The number of neurons in the input and output layers is representative of the number of independent variables (input) and dependent variables (output) respectively. Each of the nodes has connected weight to all the nodes in the next layer calculated to give the sum of the nodes (x) representing an activation input value function of the node. The value of x is computed first followed by computing the activation function of the node until the output nodes activation function is acquired. Hidden layer with different nodes is used to process the information received by the input nodes through activation function. In this study, a multilayer feed-forward network structure was used with three input parameters (temperature, thickness and drying time), 1–3 hidden layers and one output parameter (moisture ratio) as shown in Figure 1. A back-propagation algorithm was applied in training of the model because it is stable when a small learning rate is used and sigmoid function was used in all cases as illustrated in Equation (8) [47].

$$f(x) = \frac{1}{1 + e^{-x}} \tag{8}$$

This algorithm passed through four steps; initialization, activation, weight training and iteration to train data. In this case, the error minimization can be obtained by several procedures; gradient descent, conjugate gradient and Levenberge-Marquardt. Several methods for speeding up back-propagation algorithm have been used like using a variable learning rate and adding a momentum term. In this process, the parameters of learning rate, momentum and number of epoch were set as 0.3, 0.2 and 500, respectively. It is worth noting that the training time in this study depended on the number of iterations which was chosen to be 200. This is because at 200 iterations, the minimum error rate

was reached. The datasets were prepared by randomly dividing the data into training (70%) and testing (30%) [48,49]. The chosen hidden layer architectures were (3), (6), (9), (3, 3), (6, 6), (9, 9), (3, 3, 3), (6, 6, 6) and (9, 9, 9) matrix, where for example, (3, 3) and (3, 3, 3), represent the 2 and 3 hidden layers with 6 and 9 neurons each (Figure 1). The number of the hidden layers and neurons are affected directly by the simplicity of the ANN topology, while few numbers of hidden layers and neurons are recommended for simplicity. The software (Weka 3.6, Hamilton, New Zealand) was used to analyze the ANN model. Overall, ANN has the ability to performing the neural fitting and prediction and in this case, could be used for future predictions without the need for the neural network tools for the specific drying conditions.

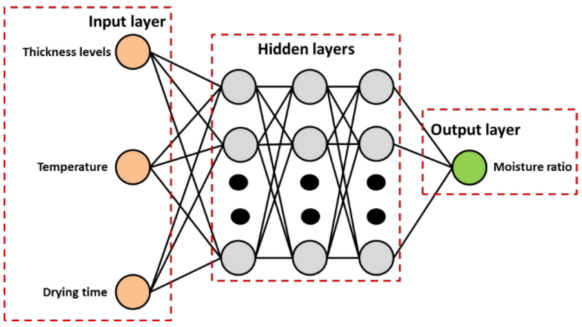

Figure 1. Artificial Neural networks topology with three hidden layers and different number of neurons.

2.7.2. Support Vector Machine

Support Vector Machine (SVM) is a supervised learning model which combines theoretical solutions with numerical algorithms used for classification and regression methods [50]. In 1999, Vapnik [51] developed the SVM algorithm and other important feature information and patterns. SVM as a regression method is considered an effective approach due to its capability of capturing non-linear relationships in the feature space.

The SVM used for the moisture ratio values was determined by the SMOreg sequence in the Waikato Environment for Knowledge Analysis (WEKA) software, whereby, the SMOreg implements SVM for regression. In this regard, the parameters of SVM learned by setting the RegOptimizer with ReqSMOImproved as a learning algorithm [52]. Figure 2 shows the workflow of using the SVM according to ReqSMOImproved learning algorithm.

The three input variables used for the SVM model were temperature, thickness and drying time with the output as the moisture ratio. Two filter types were applied, namely normalize and standardize in order to determine how/if the data need to be transformed. Additionally, three different kernel models: polynomial, Pearson universal and Radial Basis Function (RBF) were used to construct the predictive model of the calculated moisture ratio values. The data required to be optimized in the three kernels' parameters for maximum performance were obtained using the Grid Search technique. Similar to ANN, the number of iterations used was 200 due to the minimum error rate limit. The three kernels' parameters were computed mathematically as described in Equations (9)–(11):

$$f(x,\ y) = \frac{((x \times y) + 1)^d}{\sqrt{((x \times y) + 1)^d ((y \times y) + 1)^d}} \tag{9}$$

$$f(x,\ y) = \frac{1}{\left[1 + \left(\frac{2\times\sqrt{\|x-y\|_2\sqrt{2^{(1/\omega)}-1}}}{\sigma}\right)^2\right]^{\omega}} \tag{10}$$

$$f(x,\ y) = e^{-'\Upsilon\|(x-y)\|^2} \tag{11}$$

where x represents the feature vector, y is referred to as the label for each x, d is the degree of polynomial, ω and σ are Pearson width parameters and 'Y is the kernel dimension.

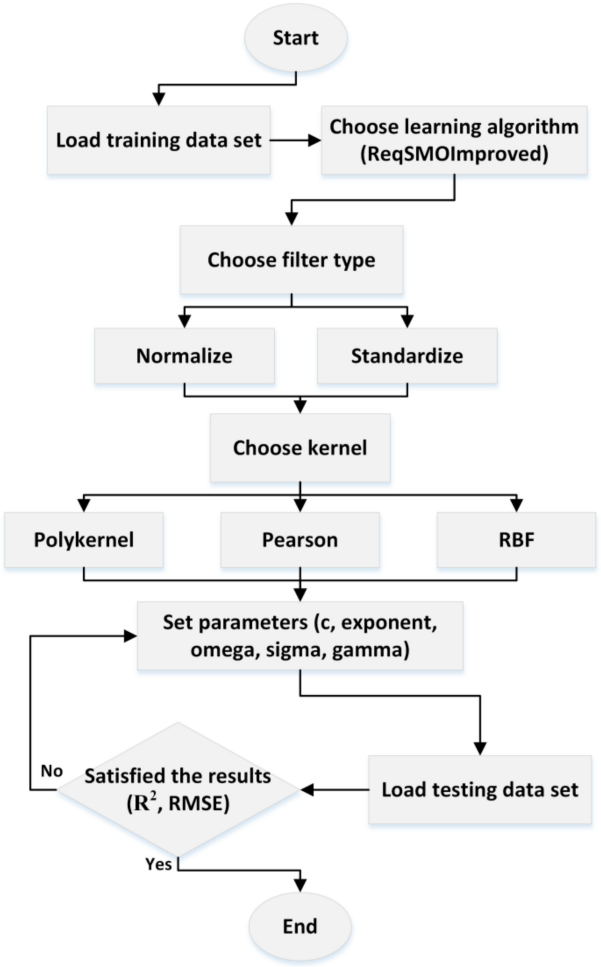

Figure 2. The workflow of support vector machine (SVM).

2.7.3. k-Nearest Neighbors

The kNN is a simple algorithm that predicts the test samples category according to the k training samples, which are the nearest neighbors to the test sample and classifies it to the category that has the largest category probability (Zhang and Zhou, 2005). kNN can select the appropriate value of k based on cross-validation and also kNN can perform distance weighting. In this study, the numbers of neighbors were used to be 3, 5, 7, 9 and 11, in order to select the best k-value in kNN based on the highest results of statistical indicators. The parameters of debug are meanSquared, crossValidate, distanceWeighting, nearestNeighbourSearchAlgorithm, windowSize and doNotCheckCapabilities did not change in Weka software. The value of the batchSize parameter in the kNN classifier was set to be 150 since the highest accuracy was observed at this value. The number of iterations was set to be 200 due to the minimum error rate. The number of decimal places used for the output of numbers in the model was 2 (numDecimalPlaces = 2).

2.8. Color Measurements

Color is one of the most important quality evaluation attributes for fruits and vegetables during drying. For the color measurements, first, the images of fresh (reference) and dried samples obtained from VD and HAD methods were captured using a smartphone camera (oppo F7, Dongguan, China). The smartphone camera is equipped with a 16 mega-pixel charged-coupled device (CCD). Samples

were put in a glass plate located on the white paper as a background during image capture for more focus and the distance between sample and smartphone camera was set-up to be 18 cm vertically. Then the images were transferred to ImageJ software for determining the color parameters: lightness (L*), redness/greenness (a*) and yellowness/blueness (b*) (http://rsb.info.nih.gov/ij/). The total color difference (ΔE) was estimated based on Equation (12). For each sample, three replications were performed.

$$E = \sqrt{(L^* - L_o^*)^2 + (a^* - a_o^*)^2 + (b^* - b_o^*)^2} \quad (12)$$

where L_o^*, a_o^* and b_o^* indicate the reference values of fresh sample.

2.9. Statistical Analysis for Mean Comparison

Statistical analysis was performed using the Statistical Analysis System software (SAS version 9.2, Institute, Inc., Cary, NC, USA). ANOVA at 5% level of significance and 95% confidence interval was performed using the Duncan test to compare the mean significant differences between quality attributes (L*, a*, b* and ΔE) for different sample thickness levels of 5 mm and 8 mm, drying time intervals between (0 and 600 minutes) and drying techniques (VD and HAD). The results were presented as mean ± standard error values. The fit accuracy of experimental data to the mathematical thin-layer and computational intelligence (ANN, SVM and kNN) models was determined by the statistical indicators: coefficient of determination (R^2) and root mean square error (RMSE) which are described mathematically in Equations (13) and (14):

$$R^2 = 1 - \frac{\sum_{i=1}^{N}\left(V_{pred} - V_{exp}\right)^2}{\sum_{i=1}^{N}\left(V_{pred} - V_m\right)^2} \quad (13)$$

$$RMSE = \sqrt{\frac{\sum_{i=1}^{N}\left(V_{pred} - V_{exp}\right)^2}{N}} \quad (14)$$

where V_{pred} is the predicted value, V_{exp} is the actual observation from experimental data, V_m is the mean of the actual observation and N is number of observations. From the values of R^2 and RMSE, the higher the value of R^2 and the lower the RMSE value, the better the goodness of fit.

3. Results and Discussion

3.1. Drying Process Behavior

The variations of moisture ratio with time for VD and HAD techniques at different temperatures (50 °C, 60 °C and 70 °C) and samples thicknesses (5 mm and 8 mm) are presented in Figure 3. From the plot, the moisture ratio of the sliced samples for all techniques decreased with an increase in drying time. The drying rates for VD and HAD methods occurred in the falling rate period. Based on Figure 3a, it is clear that the drying time thus reduces as the drying temperature increases. The moisture ratio values of 0.18 and 0.28 were determined at drying time of 170 min and temperatures of 50 ° C and 60 °C. At a drying time of 360 min at 70 °C was found the moisture ratio of 0.22. As shown in Figure 3b, as the drying time increased, for example, the moisture ratio values at 300 min at 50 °C and 70 °C were 0.44 and 0.12 respectively. Similar results were observed for HAD at samples thickness levels of 5 mm and 8 mm as illustrated in Figure 3c,d. For example, the final time found from HAD of 5 mm sample thickness at 50 °C, 60 °C and 70 °C was 420 min, 300 min and 240 min respectively. The results indicate that the moisture transfer rate from the inner layers to its surface thus increases as the drying air temperature increases. The rate of moisture evaporation at the surface of dried material to the atmosphere also increases as the temperature increase leading to a higher drying rate. The results are in agreement with other researchers on the drying behavior of various varieties of persimmon [1,2,5].

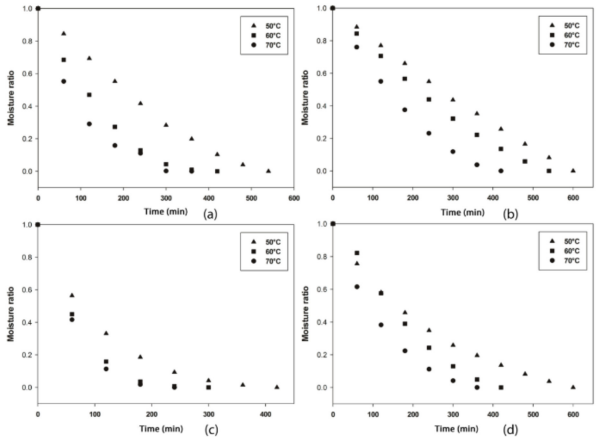

Figure 3. Drying characteristics of persimmon fruit sliced samples; (**a**) vacuum drying (VD) of sample thickness of 5 mm; (**b**) VD of 8 mm; (**c**) hot-air drying (HAD) of 5 mm; (**d**) HAD of 8 mm.

3.2. Results of Effective Moisture Diffusivity

The values of the effective moisture diffusivity (D_{eff}) are presented in Table 2. The Deff values were varied between the range of 1.417×10^{-9} m^2/s and 1.925×10^{-8} m^2/s. As it can be seen from Table 2, the D_{eff} increased significantly with increasing drying temperature from 50 °C to 70 °C. The HAD with a 5 mm thickness of persimmon samples illustrated the highest values of D_{eff} as compared to VD. The result is attributed to the increase in water molecules activity at higher temperatures leading to higher moisture diffusivity [53]. Moreover, the D_{eff} values of samples thickness of 5 mm were higher than samples of 8 mm thickness for VD and HAD drying techniques (Table 2). This is because of the increased heat arising from the increase in drying temperature of the product resulting to the water molecules activities compared to samples of bigger thickness. The values of D_{eff} obtained in this study were within the general range of 10^{-6} to 10^{-12} m^2/s for drying of food materials [5,54]. The values of D_{eff} are agreement with published works for strawberry drying ($2.40–12.1 \times 10^{-9}$ m^2/s), apple drying ($2.27–4.97 \times 10^{-10}$ m^2/s), persimmon slices ($2.60–5.40 \times 10^{-10}$ m^2/s) and pumpkin drying ($1.19–4.27 \times 10^{-9}$ m^2/s) [17,55–57].

Table 2. Values for effective moisture diffusivity, D_{eff}.

Thickness (mm)	Drying Method	D_{eff} (m^2/s)	R^2	RMSE
5	VD-50	3.316×10^{-9}	0.9647	0.5564
	VD-60	8.742×10^{-9}	0.9897	0.4563
	VD-70	1.330×10^{-8}	0.8094	0.3829
8	VD-50	1.417×10^{-9}	0.9670	0.6056
	VD-60	2.688×10^{-9}	0.9710	0.5708
	VD-70	2.959×10^{-9}	0.9786	0.5273
5	HAD-50	9.221×10^{-9}	0.9900	0.3632
	HAD-60	1.712×10^{-8}	0.9956	0.3280
	HAD-70	1.925×10^{-8}	0.9991	0.3461
8	HAD-50	2.905×10^{-9}	0.9314	0.4644
	HAD-60	4.834×10^{-9}	0.9811	0.5641
	HAD-70	7.890×10^{-9}	0.9888	0.4395

3.3. Results of Activation Energy

The activation energy (*Ea*) of persimmon fruit samples was calculated from the values of effective moisture diffusivity, D_{eff}. The relationship between *Ea* and D_{eff} was described by an Arrhenius-type equation (Equation (6)). The values of activation energy were obtained by plotting

$ln(D_{eff})$ versus 1/(T + 273.15) for VD and HAD methods. The activation energy is equal to the slope times the universal gas constant (R) as shown in Figure 4. The activation energy values for the VD and HAD for samples thicknesses (5 mm and 8 mm) were further estimated as given in Table 3. The values of *Ea* for the VD method were 64.2895 kJ/mol and 34.1785 kJ/mol for 5 mm and 8 mm respectively. While for the HAD method, the *Ea* was 34.1560 kJ/mol at 5 mm thickness, and that of 8 mm was 46.0715 kJ/mol at temperatures between 50 °C and 70 °C. The results found in this study are similar to those reported for persimmon sliced samples with activation energy between 30.64 and 43.26 kJ/mol for blanched and control respectively [5]. The *Ea* values of persimmon samples dried using VD and HAD methods were consistent with those in the literature for different fruits and vegetables, for example,30.46–35.57 kJ/mol in strawberry, 25.26–72.47 kJ/mol in yams and 22.66–30.92 kJ/mol in apples [17,58,59]. The values of *Ea* were within the acceptable range from 12.7 to 110 kJ/mol for various food materials [60].

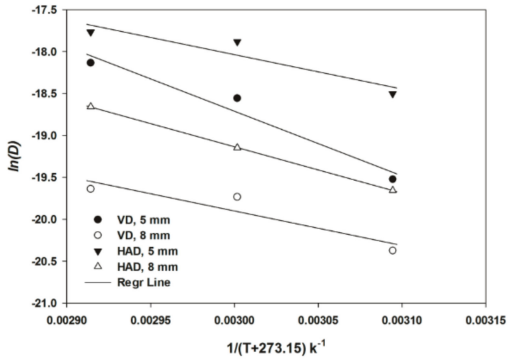

Figure 4. Arrhenius-type relationship of effective moisture diffusivity versus temperature for VD and HAD methods at different samples thickness levels.

Table 3. Activation energy of persimmon fruit samples for VD and HAD at different thickness levels.

Drying Method	R^2	E_a (kJ/mol)
VD-5 mm	0.9577	64.2895
VD-8 mm	0.8583	34.1785
HAD-5 mm	0.8774	34.1560
HAD-8 mm	0.9999	46.0715

3.4. Comparison of Mathematical Thin-Layer Models

The mathematical thin-layer models were used to describe the drying kinetics of persimmon fruit samples for VD and HAD methods. Tables 4–7 show the selected mathematical models that fitted the experimental moisture content data in relation to samples thickness levels of 5 mm and 8 mm. Although all the selected ten models adequately fitted the experimental data, the logarithmic model sufficiently described the drying kinetics of persimmon samples with R^2 values (> 0.9900) and lowest RMSE values (< 0.0200) for VD technique at all drying temperatures as given in Table 4. Similar results were obtained for VD at 8 mm thickness indicating that the logarithmic model showed the best model to fit the experimental data with the highest R^2 of > 0.0990 and the lowest RMSE of < 0.0100 at all the three temperatures (50 °C, 60 °C and 70 °C). For HAD technique, the Page, Logarithmic, Midilli et.al and Hii et al. models significantly described the drying kinetics of persimmon samples of thicknesses (5 mm and 8 mm) with R^2 of more than 0.9990 and lowest RMSE of less than 0.0010 (Tables 6 and 7). For example, the validation of the logarithmic model by comparing the predicted moisture data and those obtained from the experiments is shown in Figure 5. The moisture ratio data predicted using the logarithmic model lied closely along a straight regression line for different drying conditions indicating the suitability of the model for describing the VD and HAD behaviors of persimmon fruit samples. Onwude et al. [61] also reported the adequacy of page, logarithmic, Midilli et al. and Hii et al. models for predicting the drying kinetics of sweet potato. Similarly, Younis et al. [62] indicated the

appropriateness of page, logarithmic, Midilli et al. and Hii et al. models for describing the drying performance of garlic slices.

Table 4. Statistical evaluation of the mathematical drying models for persimmon samples of 5 mm thickness for VD.

Drying Temperature (°C)	Model No.	Model Parameters	R^2	RMSE
50	1	k = 0.2491	0.9577	0.0682
	2	k = 0.1224, n = 1.4734	0.9940	0.2559
	3	k = 0.2259, n = 1.1031	0.9577	0.0762
	4	a = 1.5532, k= 0.1229, c = −0.5369	0.9980	0.0146
	5	a = 0.5606, k_1 = 0.2663, b = 0.5108, k_2 = 0.2663	0.9650	0.0620
	6	a = 0.6224, k_0 = 0.2491, k_1 = 0.4003	0.9577	0.0815
	7	a = 1.0713, k = 0.2663	0.9650	0.0693
	8	a = 0.3715, k = 0.2663, b = 0.3610, g = 0.2663, c = 0.3388, h = 0.2663	0.9650	0.0620
	9	a = 1.0177, k = 0.1639, b = -0.0287	0.9976	0.0194
	10	a = 0.4916, k_1 = 0.1068, b = 0.4821, k_2 = 0.1068, n = 1.5424	0.9948	0.0339
60	1	k = 0.4503	0.9821	0.0457
	2	k = 0.3292, n = 1.3069	0.9960	0.0217
	3	k = 0.4097, n = 1.0990	0.9821	0.0527
	4	a = 1.1435, k = 0.3445, c = −0.1331	0.9964	0.0206
	5	a = 0.5347, k_1 = 0.4632, b = 0.4988, k_2 = 0.4632	0.9836	0.0438
	6	a = 0.6046, k_0 = 0.4503, k_1 = 0.7448	0.9821	0.0577
	7	a = 1.0335, k = 0.4632	0.9836	0.0505
	8	a = 0.3531, k = 0.4632, b = 0.3503, g = 0.4632, c = 0.3300, h = 0.4632	0.9836	0.0438
	9	a = 1.0125, k = 0.3867, b = -0.0143	0.9955	0.0289
	10	a = 0.4936, k_1 = 0.3194, b = 0.4955, k_2 = 0.3194, n = 1.3254	0.9961	0.0348
70	1	k = 0.6145	0.9957	0.0220
	2	k = 0.5871, n = 1.0608	0.9963	0.0205
	3	k = 0.5954, n = 1.0320	0.9957	0.0260
	4	a= 1.0325, k = 0.5613, c = −0.0345	0.9974	0.0173
	5	a = 0.5045, k_1 = 0.6171, b = 0.5003, k_2 = 0.6171	0.9958	0.0219
	6	a = 0.6832, k_0 = 0.6145, k_1 = 0.8993	0.9957	0.0290
	7	a = 1.0049, k = 0.6171	0.9958	0.0259
	8	a = 0.3329, k= 0.6171, b = 0.3408, g = 0.6171, c = 0.3312, h = 0.6171	0.9958	0.0219
	9	a = 0.9985, k = 0.5811, b = −0.0054	0.9975	0.0223
	10	a = 0.4869, k_1 = 0.5862, b = 0.5122, k_2 = 0.5862, n = 1.0617	0.9963	0.0383

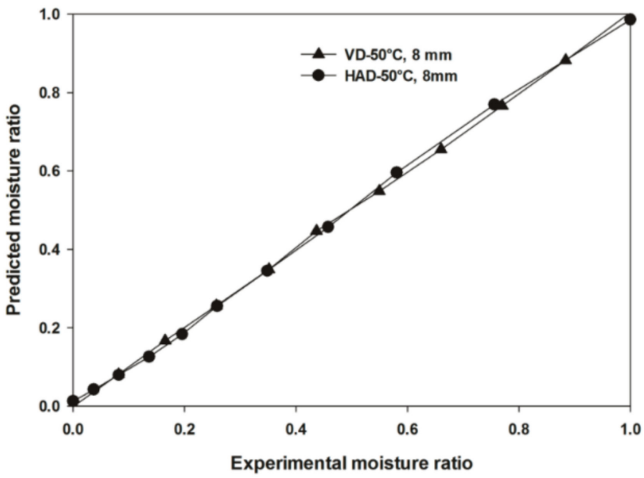

Figure 5. Predicted versus experimental moisture ratio data for logarithmic model at 50 °C and 8 mm samples thickness for VD and HAD methods.

Table 5. Statistical evaluation of the mathematical drying models for persimmon samples of 8 mm thickness for VD.

Drying Temperature (°C)	Model No.	Model Parameters	R^2	RMSE
50	1	k= 0.1854	0.9420	0.0765
	2	k = 0.0754, n = 1.5266	0.9878	0.0350
	3	k = 0.1702, n = 1.0897	0.9420	0.0846
	4	a = 2.8487, k = 0.0435, c = −1.8449	0.9998	0.0040
	5	a = 0.5626, k_1 = 0.2010, b = 0.5161, k_2 = 0.2010	0.9522	0.0694
	6	a = 0.5761, k_0 = 0.1854, k_1 = 0.3219	0.9420	0.0897
	7	a = 1.0787, k = 0.2010	0.9522	0.0768
	8	a = 0.3734, k = 0.2010, b = 0.3626, g = 0.2010, c = 0.3427, h = 0.2010	0.9522	0.0694
	9	a = 1.0046, k = 0.0795, b = −0.0456	0.9998	0.0050
	10	a = 0.4864, k_1 = 0.0580, b = 0.4751, k_2 = 0.0580, n = 1.6487	0.9896	0.0439
60	1	k = 0.2355	0.9579	0.0667
	2	k = 0.1183, n = 1.4480	0.9921	0.0288
	3	k = 0.2152, n = 1.0947	0.9579	0.0746
	4	a = 1.6897, k = 0.1027, c = −0.6819	0.9994	0.0076
	5	a = 0.5557, k_1 = 0.2512, b = 0.5109, k_2 = 0.2512	0.9646	0.0611
	6	a = 0.6343, k_0 = 0.2355, k_1 = 0.3713	0.9579	0.0797
	7	a = 1.0665, k = 0.2512	0.9646	0.0683
	8	a = 0.3682, k = 0.2512, b = 0.3594, g = 0.2512, c = 0.3389, h = 0.2512	0.9646	0.0611
	9	a = 1.0092, k = 0.1438, b = −0.0323	0.9992	0.0107
	10	a = 0.4885, k_1 = 0.1009, b = 0.4817, k_2 = 0.1009, n = 1.5277	0.9931	0.0382
70	1	k = 0.3601	0.9736	0.0548
	2	k = 0.2336, n = 1.3657	0.9955	0.0228
	3	k = 0.3303, n = 1.0903	0.9736	0.0633
	4	a = 1.3017, k = 0.2238, c = −0.2918	0.9987	0.0120
	5	a = 0.5419, k_1 = 0.3756, b = 0.5052, k_2 = 0.3756	0.9768	0.0513
	6	a = 0.6891, k_0 = 0.3601, k_1 = 0.5225	0.9736	0.0693
	7	a = 1.0470, k = 0.3756	0.9768	0.0593
	8	a = 0.3581, k = 0.3756, b = 0.3542, g = 0.3756, c = 0.3347, h = 0.3756	0.9768	0.0513
	9	a = 1.0117, k = 0.2714, b = -0.0249	0.9983	0.0177
	10	a = 0.4921, k1 = 0.2225, b = 0.4942, k_2 = 0.2225, n = 1.3937	0.9957	0.0363

Table 6. Statistical evaluation of the mathematical drying models for persimmon samples of 5 mm thickness for HAD.

Drying Temperature (°C)	Model No.	Model Parameters	R^2	RMSE
50	1	k = 0.5737	0.9986	0.0120
	2	k = 0.5514, n = 1.0481	0.9990	0.0103
	3	k = 0.5582, n = 1.0277	0.9986	0.0139
	4	a = 1.0228, k = 0.5349, c = −0.0255	0.9998	0.0047
	5	a = 0.5027, k_1 = 0.5753, b = 0.5005, k_2 = 0.5753	0.9987	0.0120
	6	a = 0.6842, k_0 = 0.5737, k_1 = 0.8384	0.9986	0.0152
	7	a = 1.0032, k = 0.5753	0.9987	0.0138
	8	a = 0.3315, k = 0.5753, b = 0.3405, g = 0.5753, c = 0.3313, h = 0.5753	0.9987	0.0120
	9	a= 0.9980, k = 0.5505, b= −0.0035	0.9998	0.0059
	10	a = 0.4894, k_1 = 0.5493, b = 0.5083, k_2 = 0.5493, n= 1.0503	0.9990	0.0167
60	1	k = 0.8838	0.9957	0.0235
	2	k = 0.7945, n = 1.2519	0.9998	0.0047
	3	k = 0.8213, n = 1.0762	0.9957	0.0288
	4	a = 1.0409, k = 0.8064, c = −0.0359	0.9982	0.0152
	5	a = 0.5142, k_1 = 0.8898, b = 0.4950, k_2 = 0.8898	0.9958	0.0232
	6	a = 0.6039, k_0 = 0.8838, k_1 = 1.4636	0.9957	0.0333
	7	a = 1.0092, k = 0.8898	0.9958	0.0284
	8	a = 0.3401, k= 0.8898, b = 0.3409, g = 0.8898, c = 0.3282, h = 0.8898	0.9958	0.0232
	9	a = 1.0058, k = 0.8451, b = −0.0064	0.9978	0.0240
	10	a = 0.4975, k_1 = 0.7941, b = 0.5022, k_2 = 0.7941, n = 1.2522	0.9998	0.0117
70	1	k = 0.9781	0.9943	0.0284
	2	k = 0.8745, n = 1.3348	0.9999	0.0031
	3	k = 0.8897, n = 1.0994	0.9943	0.0367
	4	a = 1.0564, k = 0.8581, c = −0.0522	0.9979	0.0171
	5	a = 0.5158, k_1 = 0.9840, b = 0.4928, k_2 = 0.9840	0.9944	0.0281
	6	a = 0.5740, k_0 = 0.9781, k_1 = 1.7039	0.9943	0.0449
	7	a = 1.0086, k = 0.9840	0.9944	0.0363
	8	a = 0.3409, k = 0.9840, b = 0.3408, g = 0.9840, c = 0.3270, h = 0.9840	0.9944	0.0281
	9	a = 1.0047, k = 0.9118, b = −0.0110	0.9974	0.0301
	10	a = 0.4973, k_1 = 0.8743, b = 0.5026, k_2 = 0.8743, n = 1.3349	0.9999	-

Table 7. Statistical evaluation of the mathematical drying models for persimmon samples of 8 mm thickness for HAD.

Drying Temperature (°C)	Model No.	Model Parameters	R^2	RMSE
50	1	k = 0.2797	0.9925	0.0264
	2	k = 0.2448, n = 1.0909	0.9946	0.0225
	3	k = 0.2702, n = 1.0350	0.9925	0.0292
	4	a = 1.0943, k = 0.2204, c = −0.1083	0.9989	0.0099
	5	a = 0.5092, k_1 = 0.2828, b = 0.5022, k_2 = 0.2828	0.9927	0.0261
	6	a = 0.6403, k_0 = 0.2797, k_1 = 0.4368	0.9925	0.0310
	7	a = 1.0114, k = 0.2828	0.9927	0.0288
	8	a = 0.3350, k= 0.2828, b = 0.3444, g = 0.2828, c = 0.3320, h = 0.2828	0.9927	0.0261
	9	a = 0.9876, k = 0.2407, b = −0.0080	0.9992	0.0100
	10	a = 0.4845, k_1 = 0.2343, b = 0.5018, k_2 = 0.2343, n = 1.1112	0.9948	0.0299
60	1	k = 0.3411	0.9622	0.0670
	2	k = 0.1887, n = 1.4915	0.9979	0.0157
	3	k = 0.3134, n = 1.0882	0.9622	0.0774
	4	a = 1.3969, k = 0.1992, c = −0.3693	0.9956	0.0229
	5	a = 0.5562, k_1 = 0.3624, b = 0.5121, k_2 = 0.3624	0.9689	0.0608
	6	a = 0.6258, k_0 = 0.3411, k_1 = 0.5450	0.9622	0.0847
	7	a = 1.0684, k = 0.3624	0.9689	0.0702
	8	a = 0.3669, k = 0.3624, b = 0.3610, g = 0.3624, c = 0.3405, h= 0.3624	0.9689	0.0608
	9	a = 1.0289, k= 0.2489, b = −0.0294	0.9949	0.0313
	10	a = 0.4986, k_1 = 0.1849, b = 0.4961, k_2 = 0.1849, n = 1.5034	0.9980	0.0254
70	1	k = 0.5139	0.9942	0.0255
	2	k = 0.4559, n = 1.1338	0.9972	0.0177
	3	k = 0.4882, n = 1.0527	0.9942	0.0302
	4	a = 1.0830, k = 0.4234, c = -0.0857	0.9998	0.0044
	5	a = 0.5125, k_1 = 0.5195, b = 0.4998, k_2= 0.5195	0.9944	0.0251
	6	a = 0.6353, k_0 = 0.5139, k_1 = 0.8089	0.9942	0.0338
	7	a = 1.0123, k = 0.5195	0.9944	0.0296
	8	a = 0.3385, k = 0.5195, b = 0.3431, g = 0.5195, c = 0.3307, h = 0.5195	0.9944	0.0251
	9	a = 0.9984, k = 0.4570, b = −0.0112	0.9999	0.0053
	10	a = 0.4915, k_1 = 0.4516, b = 0.5040, k_2= 0.4516, n= 1.1393	0.9972	0.0329

3.5. Results of Artificial Neural Network

The parameters namely time, temperature and samples thickness were used to predict moisture ratio using ANN model for VD and HAD techniques. Tables 8 and 9 show the statistical results with respect to training and validation of the multilayer feed-forward network structure of samples drying data for VD and HAD. The training data set were used to assess the optimum number of neurons and hidden layers for multilayer neural network modelling for determining the best predictive power. For VD, it was found that the architecture with 1 and 2 hidden layers with 9 and 12 (6, 6 neurons), obtained the best results for training set (R^2 = 0.9991) and test set (R^2 = 0.9881) as compared to those of 1 hidden layer (3 and 6 neurons), 2 hidden layers (6 and 18 neurons) and 3 hidden layers (9, 18 and 27 neurons), respectively (Table 8). Moreover, the networks were found to be susceptible to the number of neurons in their hidden layers. Thus, smaller neurons led to under fitting, while too many neurons contributed to overfitting. In addition, Figure 6 showed the predicted and experimental moisture ratio values for the optimal ANN for training and testing sets.

Table 9 presented the statistical results of drying kinetics of persimmon samples for the ANN model using HAD. Similar to VD, the results showed that the architecture with 1 and 2 hidden layers with 9 and 6 (3, 3) neurons, obtained the best results as compared to those of 1 hidden layer (3 and 6 neurons), 2 hidden layers (12 and 18 neurons) and 3 hidden layers (9, 18 and 27 neurons), respectively. The highest result of R^2 values found for training and testing set were 0.9994 and 0.9979, respectively. Therefore, to compare the results obtained from the thin-layer mathematical models and ANN results, it can be seen that the ANN model is very close to the highest model in the theoretical mathematical models with R^2 and RMSE values of 0.9994 and 0.0124, respectively as compared to those of the logarithmic model (R^2 = 0.9998 and RMSE = 0.0044). Additionally, the predicted and experimental moisture ratio values for the optimal ANN for training and testing data sets are illustrated in Figure 7.

Zenoozian et al. [63] demonstrated that 1 and 2 hidden layers and 30 neurons for ANN adequately predicted the moisture changes of pumpkin during osmotic dehydration. ANN with 1 and 2 hidden layers have also been successful in predicting the drying behavior of other fruits and vegetables such as pepper, apple slices, mushroom during microwave-vacuum drying [36,64,65].

Table 8. Statistical results of drying kinetics of persimmon fruit samples for the artificial neural network (ANN) model using VD.

No. Hidden Layer	No. Neurons	Training		Testing	
		R^2	RMSE	R^2	RMSE
1	3	0.9979	0.0249	0.9791	0.0696
1	6	0.9990	0.0245	0.9794	0.0692
1	9	0.9991	0.0213	0.9812	0.0671
2	3, 3	0.9981	0.0209	0.9820	0.0658
2	6, 6	0.9978	0.0237	0.9881	0.0572
2	9, 9	0.9976	0.0312	0.9848	0.0800
3	3, 3, 3	0.9980	0.0275	0.9803	0.0704
3	6, 6, 6	0.9982	0.0264	0.9854	0.0576
3	9, 9, 9	0.9987	0.0269	0.9866	0.0661

Table 9. Statistical results of drying kinetics of persimmon samples for the ANN model using HAD.

No. Hidden Layer	No. Neurons	Training		Testing	
		R^2	RMSE	R^2	RMSE
1	3	0.9952	0.0655	0.9885	0.0557
1	6	0.9962	0.0296	0.9882	0.0878
1	9	0.9992	0.0183	0.9979	0.0351
2	3, 3	0.9994	0.0124	0.9983	0.0281
2	6, 6	0.9975	0.0529	0.9943	0.0605
2	9, 9	0.9989	0.0297	0.9979	0.0459
3	3, 3, 3	0.9518	0.1348	0.8025	0.3419
3	6, 6, 6	0.9969	0.0344	0.9947	0.0649
3	9, 9, 9	0.9983	0.0233	0.9952	0.0431

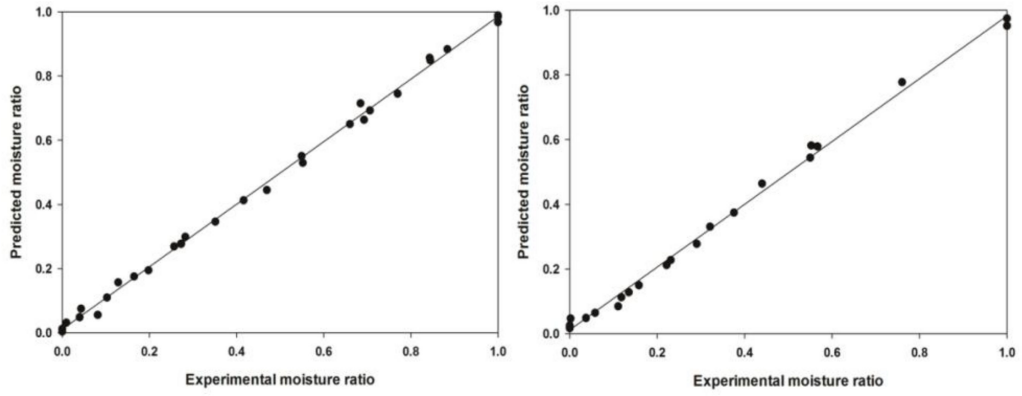

Figure 6. Predicted and experimental moisture ratio using VD from training and testing data set of ANN model.

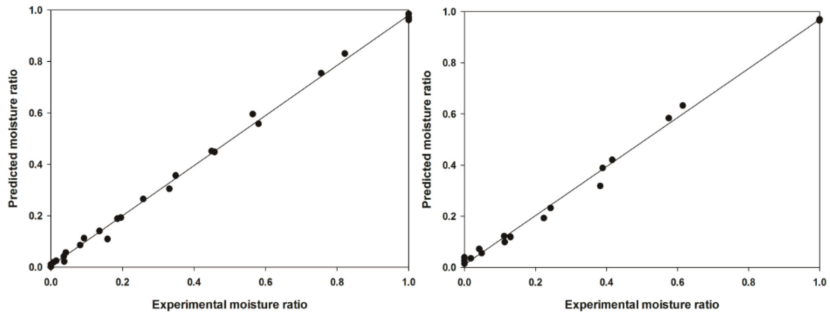

Figure 7. Predicted and experimental moisture ratio using HAD from training and testing data set of ANN.

3.6. Results of Support Vector Machine

The statistical results related to the training and validation of the SVM of persimmon drying experimental data using VD and HAD are given in Tables 10 and 11. Similar to the ANN model, the training data set was used to evaluate the best filter and kernel type modeling for determining the best predictive power. For VD, the training data set at standardize filter with Pearson universal kernel type found the best result of R^2 and RMSE values of 1.0000 and 0.0004 as compared to those of normalize with polynomial, Pearson universal kernel and RBF kernel and also standardize with polynomial and RBF kernel, respectively. For the testing data set, standardize filter with polynomial kernel type obtained the best results for R^2 and RMSE values of 0.9996 and 0.1213 (Table 10).

Table 10. Statistical results of drying kinetics of persimmon samples for SVM model using VD method.

Filter Type	Kernel Type	Training		Testing	
		R^2	RMSE	R^2	RMSE
Normalize	Polynomial kernel	0.9672	0.0904	0.9234	0.1339
Normalize	Pearson universal kernel	1.0000	0.0014	0.9564	0.1041
Normalize	RBF kernel	0.9998	0.0067	0.9575	0.1000
Standardize	Polynomial kernel	0.9672	0.0903	0.9996	0.1213
Standardize	Pearson universal kernel	1.0000	0.0004	0.9258	0.2174
Standardize	RBF kernel	0.9999	0.0040	0.9577	0.1042

Table 11. Statistical results of drying kinetics of persimmon samples for SVM model using HAD method.

Filter Type	Kernel Type	Training		Testing	
		R^2	RMSE	R^2	RMSE
Normalize	Polynomial kernel	0.8712	0.1697	0.8797	0.1612
Normalize	Pearson universal kernel	0.9996	0.0103	0.9680	0.0862
Normalize	RBF kernel	0.9980	0.0233	0.9674	0.0871
Standardize	Polynomial kernel	0.9339	0.1337	0.8797	0.1612
Standardize	Pearson universal kernel	1.0000	0.0005	0.8933	0.2308
Standardize	RBF kernel	1.0000	0.0004	0.9690	0.0912

However, for HAD, the standardize filter type with RBF kernel obtained the best results for training and testing data set of R^2 and RMSE values of 1.0000, 0.0004, 0.9690 and 0.0912 respectively (Table 11). From the results, it is clear that the SVM model showed the highest results as compared to the theoretical mathematical models and also ANN (Tables 7 and 9). Few studies used SVM as a model in drying techniques. Das and Akpinar [50] applied SVM to investigate pear drying performance by different ways of convective heat transfer. The authors applied normalization and standardization filter to the target attribute with three kernel models (polynomial kernel, Pearson universal kernel

and RBF kernel). They found that the polynomial kernel showed the lowest RMSE of value 0.3351. This indicates that the applied algorithm for SVM prediction for the moisture ratio during the drying process for both VD and HAD techniques can be promised.

3.7. Results of k-Nearest Neighbors

Tables 12 and 13 summarized the R^2 and RMSE of kNN tool developed with training and testing data set for VD and HAD methods. For VD method, the prediction model developed using a k-value of 3, produced the highest results for training and testing data set of R^2 values of 0.9327 and 0.8782 and lowest RMSE values of 0.1271 and 0.1829 respectively. Meanwhile, k-values of 11 and 9 indicated the lowest R^2 values of 0.8355 and 0.5638 and the highest RMSE values of 0.2214 and 0.6399 for training and testing data set, respectively (Table 12). For HAD technique, the results of the training set showed R^2 values between 0.6347 and 0.8638 and RMSE values between 0.2145 and 0.2907. The k-value of 7 showed the highest result compared to other k-values (3, 5, 9 and 11). The prediction model developed using the testing data set indicated R^2 values of ranging from 0.4877 to 0.7873 and RMSE values from 0.2385 to 0.3099. The k-value of 5 showed the highest values (Table 13).

Table 12. Statistical results of drying kinetics of persimmon samples for k nearest neighbors (kNN) model using VD method.

k	Training		Testing	
	R^2	RMSE	R^2	RMSE
3	0.9327	0.1271	0.8782	0.1829
5	0.9209	0.1548	0.7881	0.2320
7	0.8969	0.1730	0.6123	0.2799
9	0.8383	0.2059	0.5638	0.2877
11	0.8355	0.2214	0.6399	0.6399

Table 13. Statistical results of drying kinetics of persimmon for kNN model using HAD method.

k	Training		Testing	
	R^2	RMSE	R^2	RMSE
3	0.7923	0.2143	0.6819	0.2510
5	0.8135	0.2253	0.7873	0.2385
7	0.8638	0.2320	0.7160	0.2673
9	0.6347	0.2860	0.4877	0.3099
11	0.7101	0.2907	0.7484	0.2955

3.8. Comparison between Computational Intelligence and Mathematical Thin-Layer Models

The highest results obtained from the computational intelligence models (ANN, SVM and kNN) and the top three mathematical thin-layer models (page, logarithmic and Midilli et al.) for moisture ratio prediction are summarized in Table 14. The R^2 value of 0.9991 and RMSE value of 0.0213 at 1 hidden layer with 9 neurons by applying ANN model showed the best results for VD method. For the HAD method applying ANN model, the R^2 value of 0.9994 and RMSE value of 0.0124 were found. For kNN, the results of R^2 and RMSE were 0.9327, 0.1271, 0.8638 and 0.2320 for VD and HAD respectively. On the other hand, the mathematical thin-layers modelling found the range of R^2 values from 0.9963 to 0.9999 and RMSE from 0.0205 to 0.0031 for both VD and HAD methods.

Table 14. Statistical results of drying kinetics of persimmon samples for computational intelligence and mathematical thin-layer models using VD and HAD.

Model		VD		HAD	
		R^2	RMSE	R^2	RMSE
Computational intelligence	ANN	0.9991	0.0213	0.9994	0.0124
	SVM	1.0000	0.0004	1.0000	0.0004
	kNN	0.9327	0.1271	0.8638	0.2320
Mathematical model	Page	0.9963	0.0205	0.9999	0.0031
	Logarithmic	0.9998	0.0040	0.9998	0.0047
	Midilli et al.	0.9998	0.0050	0.9999	0.0053

It can be seen that the prediction of moisture ratio with the model developed using SVM gave the highest R^2 and the lowest RMSE values of 1.0000 and 0.0004 compared to the models developed using other computational intelligence methods (ANN and kNN) and mathematical thin-layers models; page, logarithmic and Midilli et al. (Table 14). The results indicate that SVM gave the best results which are in agreement with the findings of prior studies [19,66] that used SVM as a data prediction method to improve outcomes. In summary, the results from this study demonstrate the application of computational intelligence methods for the drying processes of persimmon samples at different conditions. Thus, applying computational intelligence methods in drying generally improves the drying performance by controlling the drying input parameters for optimizing energy, quality and production cost.

3.9. Results of Color Measurements

The color properties of persimmon samples of 5 mm and 8 mm thickness for VD and HAD methods were determined based on the change in color parameters of L *, a * and b * and the total color change ΔE as given in Table 15. It can be seen clearly from Table 4 that the lightness (L *) of persimmon samples dried using VD and HAD methods decreased significantly ($P \leq 0.05$) compared to the fresh samples. However, there was no significant difference between the lightness of samples using HAD-60 for 5 mm and HAD-60 and HAD-70 for 8mm, with those of the fresh samples. The VD method significantly ($P \leq 0.05$) reduced the lightness of samples compared to HAD. The VD-70 for 8 mm showed the lowest lightness value of 33.479 ± 6.888. The redness/greenness (a *) of all dried persimmon samples reduced significantly ($P \leq 0.05$) compared to fresh samples, except VD-50, which resulted in higher a* value than the fresh. Generally, the values of redness/greenness (a *) found using HAD were lower than the values found using VD. The lowest value of redness/greenness (a *) was found to be 6.032 ± 1.740 using HAD-60. Similar results were found for the yellowness/blueness (b *), where all dried persimmon samples were reduced significantly ($P \leq 0.05$) compared to fresh samples, except HAD-60, which resulted in higher b* than the fresh. In addition, there was no significant difference between the b* fresh samples with those of dried samples using VD-50, VD-60, VD-70 for 5 mm; VD-60 for 8 mm; HAD-50, HAD-60, HAD-70 for 5 mm and HAD-50, HAD-60, HAD-70 for 8 mm. Dried samples using VD-50 and VD-70 methods for 8 mm showed different groups of values of 45.250 ± 2.542 and 38.733 ± 6.948 respectively. The values of total color change using VD method showed higher values compared to the HAD method for the persimmon samples. The highest value was found using VD-70 for 8 mm of 38.733 ± 6.948. Generally, the change of color properties of the fresh samples under different drying methods is due to the increased sample temperature resulting from increased enzymatic and non-enzymatic chemical reactions of the product [67,68].

Table 15. Drying methods and color parameters of persimmon fruit samples.

Thickness (mm)	Drying Method	Color Properties for Different Sample Thickness			
		L *	a *	b *	ΔE
5	Fresh	61.425 ± 2.533 ^{ab}	26.282 ± 0.747 ^{b}	65.698 ± 2.126 ^{ab}	-
	VD-50	52.560 ± 3.680 ^{bc}	20.69 ± 1.95bc ^{d}	56.040 ± 3.410 ^{b}	17.790 ± 4.100 ^{bcd}
	VD-60	56.161 ± 3.476 ^{bc}	16.280 ± 3.598 ^{de}	61.073 ± 2.834 ^{ab}	15.859 ± 1.822 ^{bcd}
	VD-70	59.646 ± 0.413 ^{bc}	12.804 ± 0.764 ^{e}	62.265 ± 0.076 ^{ab}	14.568 ± 0.669 ^{cd}
8	VD-50	39.637 ± 2.554 ^{d}	31.815 ± 1.901 ^{a}	45.250 ± 2.542 ^{c}	27.069 ± 3.852 ^{ab}
	VD-60	50.341 ± 2.610 ^{c}	15.736 ± 0.868 ^{de}	55.656 ± 2.020 ^{b}	16.624 ± 1.715 ^{bcd}
	VD-70	33.479 ± 6.888 ^{d}	22.842 ± 0.784 ^{bc}	38.733 ± 6.948 ^{c}	35.875 ± 9.638 ^{a}
5	HAD-50	56.930 ± 1.152 ^{bc}	23.438 ± 0.258 ^{b}	61.762 ± 1.088 ^{ab}	9.528 ± 1.568 ^{d}
	HAD-60	60.250 ± 2.229 ^{ab}	11.684 ± 0.259 ^{e}	64.831 ± 2.231 ^{ab}	14.928 ± 0.680 ^{bcd}
	HAD-70	59.846 ± 1.149 ^{bc}	17.259 ± 1.164 ^{cde}	64.491 ± 0.750 ^{ab}	10.140 ± 0.405 ^{d}
8	HAD-50	56.301 ± 1.562 ^{bc}	20.571 ± 2.890 ^{bcd}	60.907 ± 0.971 ^{ab}	8.817 ± 0.789 ^{d}
	HAD-60	60.310 ± 1.478 ^{ab}	6.032 ± 1.740 ^{f}	69.432 ± 0.556 ^{a}	24.618 ± 2.301 ^{abc}
	HAD-70	60.781 ± 1.973 ^{ab}	11.541 ± 0.798 ^{e}	64.015 ± 1.325 ^{ab}	15.959 ± 0.876 ^{bcd}

Different letters at the same column indicates statistical difference for Duncan test, $P < 0.05$.

4. Conclusions

This study investigated the potential of using computational intelligence as a modelling tool for predicting the drying process of persimmon fruit samples. The performance of vacuum drying (VD) and hot-air-drying (HAD) techniques for drying persimmon fruit samples was evaluated. The results showed that VD and HAD had a significant effect on the drying kinetics, moisture diffusivity, activation energy and color properties of persimmon fruit samples. An increase in drying temperature and samples thickness influenced the drying kinetics and moisture diffusivity of samples. The effective moisture diffusivity and activation energy varied between 1.417×10^{-9} m^2/s and 1.925×10^{-8} m^2/s and 34.1560 kJ/mol to 64.2895 kJ/mol respectively. Persimmon fruit samples using HAD showed significant color attributes compared to VD method.

The mathematical thin-layer modelling results showed that page and logarithmic models can adequately (R^2 = 0.9999) describe the drying kinetics of persimmon fruit samples. The highest R^2 values of 0.9994, 1.0000 and 0.9327 were observed for ANN (2 hidden layers with (3, 3) neurons), SVM (standardize filter and RBF kernel) and kNN (k-value of 3) models, respectively. SVM tool as a computational intelligence method produced higher results compared to mathematical thin-layer. Therefore, SVM models are able to describe a wider range of experimental data whereas the application of theoretical models is limited to specific experimental conditions in most cases. Thus, computational intelligence models may be considered as a suitable alternative modelling method for describing the drying behavior of persimmon sliced samples. On the other hand, computational intelligence methods can be successfully applied to industrial drying processes and operations as well as online monitoring and control. However, further study is required to ascertain the suitability of ANN, SVM and kNN for predicting the nutritional composition of fruits and vegetables during drying.

Author Contributions: Conceptualization, A.Y.K. and D.H.; methodology, A.Y.K.; software, A.Y.K.; validation and investigation, A.K., K.Ç.S.; formal analysis, A.Y.K.; resources, D.H.; writing—original draft preparation, A.Y.K.; writing—review and editing, A.K., K.Ç.S., Č.M. and P.H.; supervision and project administration, D.H. All authors have read and agreed to the published version of the manuscript.

Funding: The research was funded by EU, Managing Authority of the Czech Operational Programme Research, Development and Education through the project "supporting the development of international mobility of research staff at CULS Prague", Grant Number: CZ.02.2.69/0.0/0.0/16_027/0008366. The APC was funded through the project "supporting the development of international mobility of research staff at CULS Prague".

Conflicts of Interest: The authors declare no conflict of interest.

References

1. Bozkir, H.; Rayman, A.; Serdar, E.; Metin, G.; Baysal, T. Ultrasonics—Sonochemistry influence of ultrasound and osmotic dehydration pretreatments on drying and quality properties of persimmon fruit. *Ultrason.-Sonochem.* **2019**, *54*, 135–141. [CrossRef] [PubMed]
2. Çalışkan, G.; Nur Dirim, E. Freeze drying kinetics of persimmon puree. *GIDA* **2015**, *40*, 9–14.
3. Heras, R.M.-L.; Landines, E.F.; Heredia, A.; Castelló, M.L.; Andrés, A. Influence of drying process and particle size of persimmon fibre on its physicochemical, antioxidant, hydration and emulsifying properties. *J. Food Sci. Technol.* **2017**, *54*, 2902–2912. [CrossRef]
4. Bolek, S.; Obuz, E. Quality characteristics of Trabzon persimmon dried at several temperatures and pretreated by different methods. *Turk. J. Agric. For.* **2014**, *38*, 242–249. [CrossRef]
5. Doymaz, I. Evaluation of some thin-layer drying models of persimmon slices (Diospyros kaki L). *Energy Convers. Manag.* **2012**, *56*, 199–205. [CrossRef]
6. Senthilkumar, T.; Jayas, D.S.; White, N.D.; Fields, P.; Gräfenhan, T. Detection of fungal infection and Ochratoxin A contamination in stored barley using near-infrared hyperspectral imaging. *Biosyst. Eng.* **2016**, *147*, 162–173. [CrossRef]
7. Rodríguez, J.; Clemente, G.; Sanjuan, N.; Bon, J. Modelling drying kinetics of thyme (Thymus vulgaris L.): Theoretical and empirical models, and neural networks. *Food Sci. Technol. Int.* **2013**, *20*, 13–22. [CrossRef]
8. Onwude, D.; Hashim, N.; Abdan, K.; Janius, R.; Chen, G. The potential of computer vision, optical backscattering parameters and artificial neural network modelling in monitoring the shrinkage of sweet potato (Ipomoea batatas L.) during drying. *J. Sci. Food Agric.* **2018**, *98*, 1310–1324. [CrossRef]
9. Si, X.; Wu, X.; Yi, J.Y.; Li, Z.; Chen, Q.; Bi, J.; Zhou, L. Comparison of different drying methods on the physical properties, bioactive compounds and antioxidant activity of raspberry powders. *J. Sci. Food Agric.* **2015**, *96*, 2055–2062. [CrossRef]
10. Tekin, Z.H.; Baslar, M. The effect of ultrasound-assisted vacuum drying on the drying rate and quality of red peppers. *J. Therm. Anal. Calorim.* **2018**, *132*, 1131–1143. [CrossRef]
11. Onwude, D.I.; Hashim, N.; Janius, R.B.; Nawi, N.; Abdan, K. Evaluation of a suitable thin layer model for drying of pumpkin under forced air convection. *Int. Food Res. J.* **2016**, *23*, 1173.
12. Karasu, S.; Akcicek, A.; Kayacan, S. Effects of different drying methods on drying kinetics, microstructure, color, and the rehydration ratio of minced meat. *Foods* **2019**, *8*, 216.
13. Bai, J.; Xiao, H.; Ma, H.; Zhou, C. Artificial neural network modeling of drying kinetics and color changes of ginkgo biloba seeds during microwave drying process. *J. Food Qual.* **2018**, *2018*, 1–8. [CrossRef]
14. Behroozi, N.; Tavakoli, T.; Ghassemian, H. Applied machine vision and artificial neural network for modeling and controlling of the grape drying process. *Comput. Electron. Agric.* **2013**, *98*, 205–213. [CrossRef]
15. Akoy, E.O.M. Experimental characterization and modeling of thin-layer drying of mango slices. *Int. Food Res. J.* **2014**, *21*, 7–11.
16. Erbay, Z.; Icier, F. A review of thin layer drying of foods: Theory, a review of thin layer drying of foods: Theory, modeling, and experimental results. *Food Sci. Nutr.* **2010**, *50*, 441–464.
17. Lee, G.; Hsieh, F. Thin-layer drying kinetics of strawberry fruit leather. *Trans. ASABE* **2008**, *51*, 1699–1705. [CrossRef]
18. Liu, Z.; Bai, J.; Yang, W.; Wang, J.; Deng, L. Effect of high-humidity hot air impingement blanching (HHAIB) and drying parameters on drying characteristics and quality of broccoli florets. *Dry. Technol.* **2019**, *37*, 1251–1264. [CrossRef]
19. Khaled, A.Y.; Aziz, S.A.; Bejo, S.K.; Nawi, N.M.; Abu Seman, I.A. Spectral features selection and classification of oil palm leaves infected by Basal stem rot (BSR) disease using dielectric spectroscopy. *Comput. Electron. Agric.* **2018**, *144*, 297–309. [CrossRef]
20. Zhang, R.; Ma, J. Feature selection for hyperspectral data based on recursive support vector machines. *Int. J. Remote Sens.* **2009**, *30*, 3669–3677. [CrossRef]
21. Xu, G.; Shen, C.; Liu, M.; Zhang, F.; Shen, W. A user behavior prediction model based on parallel neural network and k-nearest neighbor algorithms. *Cluster Comput.* **2017**, *20*, 1703–1715. [CrossRef]
22. Kirbas, I.; Tuncer, A.D.; Şirin, C.; Usta, H. Modeling and developing a smart interface for various drying methods of pomelo fruit (Citrus maxima) peel using machine learning approaches. *Comput. Electron. Agric.* **2019**, *165*, 104928. [CrossRef]

23. Omari, A.; Behroozi-Khazaei, N.; Sharifian, F. Drying kinetic and artificial neural network modeling of mushroom drying process in microwave-hot air dryer. *Food Process Eng.* **2018**, *41*, 1–10. [CrossRef]
24. Movagharnejad, K.; Nikzad, M. Modeling of tomato drying using artificial neural network. *Comput. Electron. Agric.* **2007**, *59*, 78–85. [CrossRef]
25. Wen, S.; Deng, M.; Inoue, A. Moisture content prediction of wood drying process using VM-based model. *Int. J. Inov. Comput. Infomation Control* **2012**, *8*, 4083–4093.
26. Beigi, M.; Ahmadi, I. Artificial neural networks modeling of kinetic curves of celeriac (Apium graveolens L) in vacuum drying. *Food Sci. Technol.* **2018**, *2061*, 1–6. [CrossRef]
27. Jafari, S.M.; Ghanbari, V.; Ganje, M.; Dehnad, D. Modeling the drying kinetics of green bell pepper in a heat pump assisted fluidized bed dryer. *J. Food Qual.* **2016**, *39*, 98–108. [CrossRef]
28. Bahmani, A.; Jafari, S.M.; Shahidi, S.-A.; Dehnad, D. Mass transfer kinetics of eggplant during osmotic dehydration by neural networks. *J. Food Process. Preserv.* **2016**, *40*, 815–827. [CrossRef]
29. Xie, C.; Li, X.; Shao, Y.; He, Y. Color measurement of tea leaves at different drying periods using hyperspectral imaging technique. *PLoS ONE* **2014**, *9*, 1–15. [CrossRef]
30. Ieracitano, C.; Adeel, A.; Morabito, F.C.; Hussain, A. A novel statistical analysis and autoencoder driven intelligent intrusion detection approach. *Neurocomputing* **2020**, *387*, 51–62. [CrossRef]
31. Ieracitano, C.; Mammone, N.; Hussain, A.; Morabito, F.C. A novel multi-modal machine learning based approach for automatic classification of EEG recordings in dementia. *Neural Netw.* **2020**, *123*, 176–190. [CrossRef] [PubMed]
32. Association of Official Analytical Chemists (AOAC). *Official Methods of Analysis of the Association of Official Analytical Chemists*, 15th ed.; United States Department of Agriculture: Rockville, MD, USA, 1990.
33. Aghbashlo, M.; Kianmehr, M.H.; Khani, S.; Ghasemi, M. Mathematical modelling of thin-layer drying of carrot. *Int. Agrophys.* **2009**, *23*, 313–317.
34. Crank, J. *The Mathematics of Diffusion*; Oxford University Press: Oxford, UK, 1979.
35. Chen, N.; Chen, M.; Fu, B.; Song, J. Far-infrared irradiation drying behavior of typical biomass briquettes. *Energy* **2017**, *121*, 726–738. [CrossRef]
36. Jafari, S.M.; Ganje, M.; Dehnad, D.; Ghanbari, V. Mathematical, fuzzy logic and artificial neural network modeling techniques to predict drying kinetics of onion. *J. Food Process. Preserv.* **2016**, *40*, 329–339. [CrossRef]
37. Gamea, G.R.; Essa, A.A. Solar drying characteristics of strawberry. *J. Food Drug Anal* **2007**, *78*, 456–464.
38. Antonio, V.; Uribe, E.; Lemus, R.; Miranda, M. Hot-air drying characteristics of Aloe vera (Aloe barbadensis Miller) and influence of temperature on kinetic parameters. *LWT-Food Sci. Technol.* **2007**, *40*, 1698–1707.
39. Kaur, K.; Singh, A.K. Drying kinetics and quality characteristics of beetroot slices under hot air followed by microwave finish drying. *African J. Agric. Res.* **2014**, *9*, 1036–1044.
40. Sacilik, K. Effect of drying methods on thin-layer drying characteristics of hull-less seed pumpkin (Cucurbita pepo L.). *J. Food Eng.* **2007**, *79*, 23–30. [CrossRef]
41. Dash, K.K.; Gope, S.; Sethi, A.; Doloi, M. Study on Thin Layer Drying Characteristics Star Fruit Slices. *Int. J. Agric. Food Sci. Technol.* **2013**, *4*, 679–686.
42. Hashim, N.; Daniel, O.; Rahaman, E. A Preliminary Study: Kinetic Model of Drying Process of Pumpkins (Cucurbita Moschata) in a Convective Hot Air Dryer. *Int. Conf. Agric. Food Eng. CAFEi2014* **2014**, *2*, 345–352. [CrossRef]
43. Zenoozian, M.S.; Feng, H.; Razavi, S.; Shahidi, F.; Pourreza, H.R. Image analysis and dynamic modeling of thin-layer drying of osmotically dehydrated pumpkin. *J. Food Process. Preserv.* **2008**, *32*, 88–102. [CrossRef]
44. Ayadi, M.; Ben Mabrouk, S.; Zouari, I.; Bellagi, A. Kinetic study of the convective drying of spearmint. *J. Saudi Soc. Agric. Sci.* **2014**, *13*, 1–7. [CrossRef]
45. Kose, U.; Arslan, A. Optimization of self-learning in computer engineering courses: An Intelligent software system supported by artificial neural network and vortex optimization algorithm. *Comput. Appl. Eng. Educ.* **2017**, *25*, 142–156. [CrossRef]
46. Haykin, S. *Neural Networks a Comprehensive Introduction*; Prentice Hall: Upper Saddle River, NJ, USA, 1999.
47. Fu, L.-M. *Neural Networks in Computer Intelligence*; Tata McGraw-Hill Education: New York, NY, USA, 2003.
48. Benkovi, M.; Mari, L.; Male, E.; Valinger, D.; Jurina, T.; Gajdo, J. Effects of drying on physical and chemical properties of root vegetables: Artificial neural network modelling. *Food Bioprod. Process.* **2020**, *119*, 148–160.
49. Onwude, D.I.; Hashim, N.; Janius, R.B.; Nawi, N.; Abdan, K. Modelling the convective drying process of pumpkin (Cucurbita moschata) using an artificial neural network. *Int. Food Res. J.* **2016**, *23*, S237–S243.

50. Das, M.; Akpınar, E. Investigation of pear drying performance by different methods and regression of convective heat transfer coefficient with support vector machine. *Appl. Sci.* **2018**, *8*, 2–16.
51. Vapnik, V.N. An overview of statistical learning theory. *IEEE Trans. Neural Netw.* **1999**, *10*, 988–999. [CrossRef]
52. Shevade, S.; Keerthi, S.S.; Bhattacharyya, C.; Murthy, K.R.K. Improvements to the SMO algorithm for SVM regression. *IEEE Trans. Neural Netw.* **2000**, *11*, 1188–1193. [CrossRef]
53. Xiao, H.; Pang, C.; Wang, L.; Bai, J.; Yang, W.; Gao, Z. Drying kinetics and quality of Monukka seedless grapes dried in an air-impingement jet dryer. *Biosyst. Eng.* **2010**, *105*, 233–240. [CrossRef]
54. Abbaspour-Gilandeh, Y.; Jahanbakhshi, A.; Kaveh, M. Prediction kinetic, energy and exergy of quince under hot air dryer using ANNs and ANFIS. *J. Sci. Food Agric.* **2020**, *8*, 594–611. [CrossRef]
55. Sacilik, K.; Elicin, A.K. The thin layer drying characteristics of organic apple slices. *J. Food Eng.* **2006**, *73*, 281–289. [CrossRef]
56. Telis-Romero, J.; Gabas, A.L.; Menegalli, F.C.; Telis, V.R.N. Drying of persimmon: Mathematical model for diffusivity as a simultaneous function of moisture content and shrinkage. In Proceedings of the Second Inter-American Drying Conference, Monteral, QC, Canada, 8–10 July 2001; pp. 243–251.
57. Tunde-Akintunde, T.Y.; Ogunlakin, G.O. Influence of drying conditions on the effective moisture diffusivity and energy requirements during the drying of pretreated and untreated pumpkin. *Energy Convers. Manag.* **2011**, *52*, 1107–1113. [CrossRef]
58. Falade, K.O.; Olurin, T.O.; Ike, E.A.; Aworh, O.C. Effect of pretreatment and temperature on air-drying of Dioscorea alata and Dioscorea rotundata slices. *J. Food Eng.* **2007**, *80*, 1002–1010. [CrossRef]
59. Meisami-asl, E.; Rafiee, S.; Keyhani, A. Tabatabaeefar, and others. Drying of apple slices (var. Golab) and effect on moisture diffusivity and activation energy. *Plant Omics* **2010**, *3*, 97.
60. Zogzas, N.P.; Maroulis, Z.B. Drying technology: An international journal moisture diffusivity data compilation in foodstuffs. *Dry. Technol. Int. J.* **2007**, *14*, 37–41.
61. Onwude, D.I.; Hashim, N.; Abdan, K.; Janius, R.; Chen, G. Modelling the mid-infrared drying of sweet potato: Kinetics, mass and heat transfer parameters, and energy consumption. *Heat Mass Transf.* **2018**, *54*, 2917–2933. [CrossRef]
62. Younis, M.; Abdelkarim, D.; El-abdein, A.Z. Saudi journal of biological sciences kinetics and mathematical modeling of infrared thin-layer drying of garlic slices. *Saudi J. Biol. Sci.* **2018**, *25*, 332–338. [CrossRef]
63. Zenoozian, M.S.; Devahastin, S.; Razavi, M.A.; Shahidi, F.; Poreza, H.R. Use of artificial neural network and image analysis to predict physical properties of osmotically dehydrated pumpkin. *Dry. Technol.* **2014**, *26*, 132–144. [CrossRef]
64. Ghaderi, A.; Abbasi, S.; Motevali, A.; Minaei, S. Comparison of mathematical models and artificial neural networks for prediction of drying kinetics of mushroom in microwave vacuum dryer. *Chem. Ind. Chem. Eng. Q.* **2012**, *18*, 283–293. [CrossRef]
65. Nadian, M.H.; Rafiee, S.; Aghbashlo, M.; Hosseinpour, S.; Mohtasebi, S.S. Continuous real-time monitoring and neural network modelling of apple slices color changes during hot air Drying. *Food Bioprod. Process.* **2014**, *94*, 1–40.
66. Samsudin, S.H.; Shafri, H.; Hamedianfar, A.; Mansor, S.B. Spectral feature selection and classification of roofing materials using field spectroscopy data. *J. Appl. Remote Sens.* **2015**, *9*, 95079. [CrossRef]
67. Nozad, M.; Khojastehpour, M.; Tabasizadeh, M. Characterization of hot-air drying and infrared drying of spearmint (Mentha spicata L) leaves. *J. Food Meas. Charact.* **2016**, *10*, 466–473. [CrossRef]
68. Onwude, D.; Hashim, N.; Janius, R.; Nawi, N.; Abdan, K. Color change kinetics and total carotenoid content of pumpkin. *Ital. J. Food Sci.* **2017**, *29*, 1–18.